Available online at www.jbr-pub.org.cn

Open Access at PubMed Central

The Journal of Biomedical Research, 2021 35(3): 179–188

JBR

Original Article

Correlation between radiologic features on contrast-enhanced CT and pathological tumor grades in pancreatic neuroendocrine neoplasms

Wenbin Xu[1,2], Han Yan[1,2], Lulu Xu[3], Mingna Li[4], Wentao Gao[1,2], Kuirong Jiang[1,2], Junli Wu[1,2], Yi Miao[1,2,✉]

[1]Pancreas Center, the First Affiliated Hospital of Nanjing Medical University, Nanjing, Jiangsu 210029, China;
[2]Pancreas Institute of Nanjing Medical University, Nanjing, Jiangsu 210029, China;
[3]Department of Radiology, [4]Department of Pathology, the First Affiliated Hospital of Nanjing Medical University, Nanjing, Jiangsu 210029, China.

Abstract

Contrast-enhanced computed tomography (CT) contributes to the increasing detection of pancreatic neuroendocrine neoplasms (PNENs). Nevertheless, its value for differentiating pathological tumor grades is not well recognized. In this report, we have conducted a retrospective study on the relationship between the 2017 World Health Organization (WHO) classification and CT imaging features in 94 patients. Most of the investigated features eventually provided statistically significant indicators for discerning PNENs G3 from PNENs G1/G2, including tumor size, shape, margin, heterogeneity, intratumoral blood vessels, vascular invasion, enhancement pattern in both contrast phases, enhancement degree in both phases, tumor-to-pancreas contrast ratio in both phases, common bile duct dilatation, lymph node metastases, and liver metastases. Ill-defined tumor margin was an independent predictor for PNENs G3 with the highest area under the curve (AUC) of 0.906 in the multivariable logistic regression and receiver operating characteristic curve analysis. The portal enhancement ratio (PER) was shown the highest AUC of 0.855 in terms of quantitative features. Our data suggest that the traditional contrast-enhanced CT still plays a vital role in differentiation of tumor grades and heterogeneity analysis prior to treatment.

Keywords: pancreatic neuroendocrine neoplasm, computed tomography, tumor grade, heterogeneity analysis

Introduction

Pancreatic neuroendocrine neoplasms (PNENs) are relatively rare tumors, accounting for less than 3% of pancreatic neoplasms[1–2]. Regarding the outcomes, the prognosis of PNENs is much better than the more common pancreatic ductal adenocarcinoma. Nevertheless, because of potentially malignant characteristics, PNENs exhibit various biological behaviors and risks of progression[3]. Apart from the traditional tumor-node-metastasis staging system, PNENs can be specifically classified into G1, G2 and G3 groups, all of which have different prognoses and require different treatment strategies based on the Ki-

✉Corresponding author: Yi Miao, Pancreas Center, the First Affiliated Hospital of Nanjing Medical University, 300 Guangzhou Road, Nanjing, Jiangsu 210029, China. Tel: +86-25-6830-6590, E-mail: miaoyi@njmu.edu.cn.

Received: 18 March 2020; Revised: 14 June 2020; Accepted: 19 June 2020; Published online: 21 August 2020

CLC number: R735.9, Document code: A

The authors reported no conflict of interests.

https://doi.org/10.7555/JBR.34.20200039

67 index and/or mitotic count, according to the tumor grading system proposed by the World Health Organization (WHO) 2010 and 2017 classification[3–4].

As the extensive use of contrast-enhanced computed tomography (CT) with high resolution, an increasing number of asymptomatic PNENs are detected incidentally[5]. Radiological examination is traditionally routine and fundamental in lesion localization, differential diagnosis, tumor staging, and assessment of curative effect. Recently, several studies investigated the imaging features in PNENs of various tumor grades; these studies suggested the possibility of using CT or magnetic resonance imaging to analyze tumor heterogeneity[6–10]. Nevertheless, the value of traditional imaging features before treatment remains to be elucidated.

Therefore, the purpose of the present study was to define the radiological characteristics of PNENs on pretreatment contrast-enhanced CT and to reveal the differences of these features between PNENs G3 and those of lower grades, so as to provide evidence for the diagnostic performance of traditional CT imaging in PNENs grade differentiation.

Patients and methods

Patients

We retrospectively reviewed the electronic clinical data system at our institution from January 2009 to December 2017. We retrieved data of patients with pathologically-proven PNENs who underwent pre-treatment abdominal contrast-enhanced CT. The inclusion criteria were as follows: (1) pathologically and immunohistochemically confirmed diagnosis of PNENs; (2) abdominal contrast-enhanced CT at our institution no longer than 1 month prior to surgery or biopsy. Exclusion criteria were as follows: (1) CT imaging data were not available (not transmitted or saved during the process of system conversion); (2) tumors could not be detected on contrast-enhanced CT images. A total of 94 patients were finally recruited from the 106 patients (***Fig. 1***). This study was approved by our institutional review board and the requirement for informed consent was waived.

Pathological assessment

All pathology slides were reviewed by a pathologist with 10 years of evaluation experience who was blinded to clinical and imaging features of these tumors. Pathological tumor grades were determined according to the WHO 2017 classification[4], including PNENs G1 (mitoses <2 per 10 high power fields [HPF] and Ki-67 index <3%) (***Fig. 2A*** and ***B***), PNENs G2 (mitoses 2 –20 per 10 HPF or Ki-67 index 3%–20%) (***Fig. 2C*** and ***D***), and PNENs G3 (mitoses >20 per 10 HPF or Ki-67 index >20%) (***Fig. 2E*** and ***F***). PNENs G3 were not further divided into PNETs G3 and PNECs because of the limited sample size.

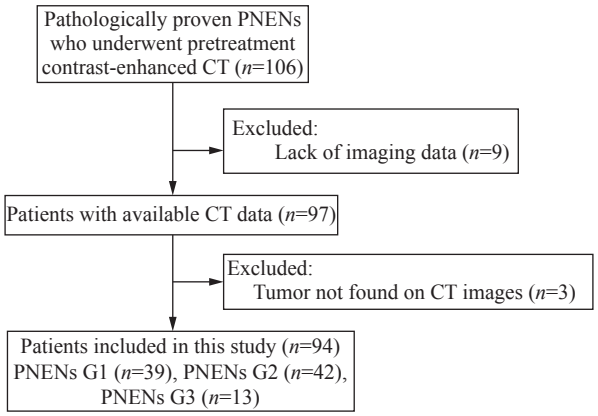

Fig. 1 **Flowchart of the inclusion process for study patients.** PNENs: pancreatic neuroendocrine neoplasms; CT: computed tomography.

CT protocol

All CT scanning was performed using the 16-slice and 64-slice MDCT (Definition AS, Siemens, Germany) following a standardized protocol. The patient's position was feet first –supine. Images of three phases (non-contrast, arterial, and portal venous) were obtained for each patient. Contrast-enhanced CT images were obtained after intravenous administration of ioversol (350 mg/mL, Jiangsu Hengrui Medicine, China) at a rate of 3.0 mL/s *via* a power injector (1.5 mL/kg), followed by a 20 mL bolus of sodium chloride. The enhanced images were obtained at the arterial phase when a threshold enhancement of 100 Hounsfield units (HU) was achieved using a bolus-tracking technique and delayed 15 seconds before scanning. The portal phase imaging was initiated 35 seconds after the completion of arterial phase scanning.

CT imaging analysis

All CT images were reevaluated on a picture archiving and communication systems workstation by two reviewers with 5 and 8 years of experience in abdominal CT interpretation who were blinded to the tumor grade. If there was any discrepancy between their evaluations, a third reviewer with more than 15 years of clinical experience made the final decision. CT features of the tumor included the following: tumor size, tumor location, tumor shape, tumor margin, heterogeneity, edge enhancement, cystic or

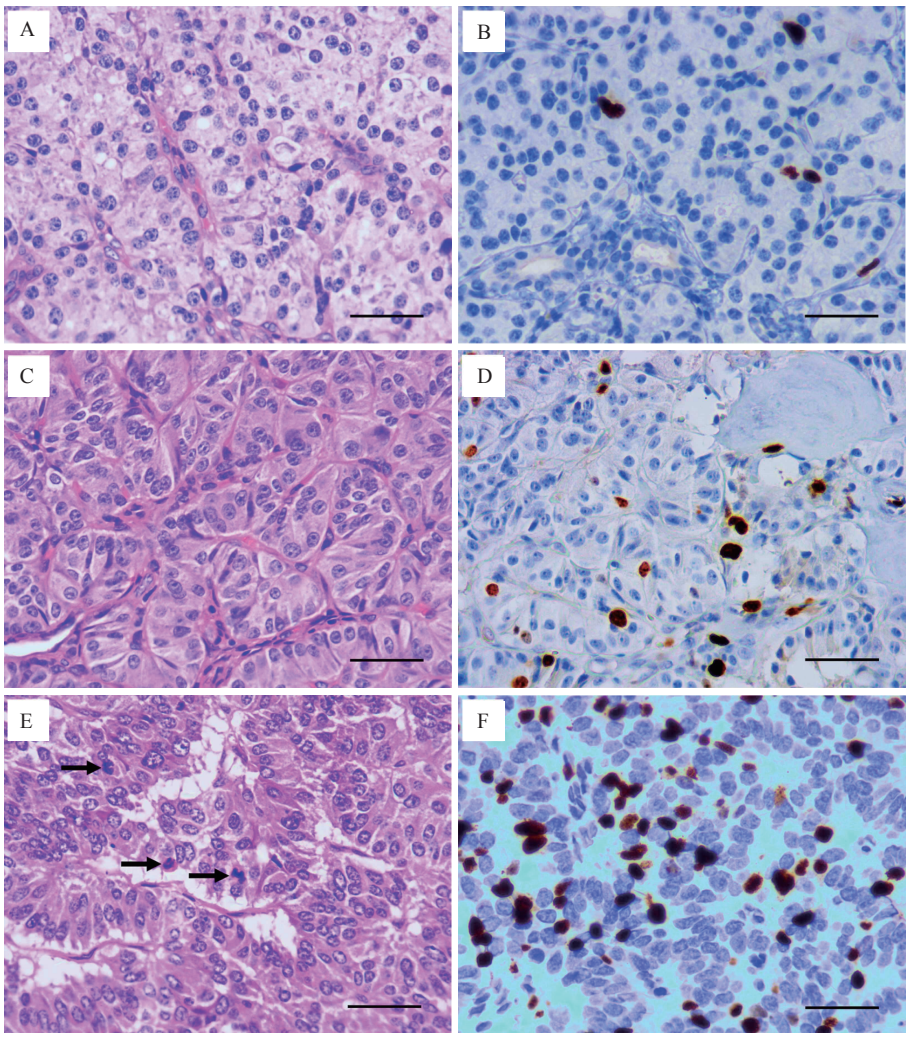

Fig. 2 **Hematoxylin-eosin and Ki-67 staining of pancreatic neuroendocrine neoplasms.** A: Mitoses <2 per 10 HPF in Hematoxylin-eosin (HE) staining of PNENs G1. B: Ki-67 index <3% in immunohistochemical (IHC) staining of PNENs G1. C: Mitoses 2–20 per 10 HPF in HE staining of PNENs G2. D: Ki-67 index 3%–20% in IHC staining of PNENs G2. E: Mitoses >20 per 10 HPF in HE staining of PNENs G3. Black arrows indicate the mitotic cells. F: Ki-67 index >20% in IHC staining of PNENs G3. Scale bar=50 μm. PNENs: pancreatic neuroendocrine neoplasms; HPF: high power field.

necrotic components, intratumoral blood vessels, vascular invasion, calcification, upstream pancreatic duct dilatation, common bile duct dilatation, lymph node metastases, liver metastases, contrast enhancement pattern in the arterial and portal phases, tumor enhancement degree in both enhanced phases, tumor-to-pancreas enhancement ratio in both enhanced phases, and peak attenuation phase.

Tumor size was determined by the largest tumor diameter on axial scans. The tumor location was classified into head/neck and body/tail. The tumor shape was divided into regular (round/oval) (***Fig. 3A***) or irregular (lobulated) (***Fig. 3B***). The tumor margin was divided into well-defined (smooth and clearly visible) (***Fig. 3C***) and ill-defined (with more than 80% of spiculation or infiltration on the perimeter of the tumor) (***Fig. 3D***). The heterogeneity was defined as uneven attenuation of the tumor on contrast-enhanced CT images (***Fig. 3E***). Edge enhancement was defined as a ring-like enhanced pattern along the edge of the tumor (***Fig. 3F***). Cystic or necrotic components within the tumor were identified as non-enhancing areas in both the arterial phase and portal phase (***Fig. 3G***). Intratumoral blood vessels were recognized as blood vessels entering the tumor parenchyma (***Fig. 3H***). The criteria for vascular invasion were occlusion, stenosis, or deformation of the main blood vessels such as celiac trunk, common hepatic artery, superior mesenteric artery/vein, splenic artery/vein, and portal vein because of tumor infiltration or compression (***Fig. 3I***). Calcification within the tumor was recorded on non-enhanced CT images. Upstream pancreatic duct dilatation was regarded as the diameter of the main pancreatic duct exceeding 3 mm, while common

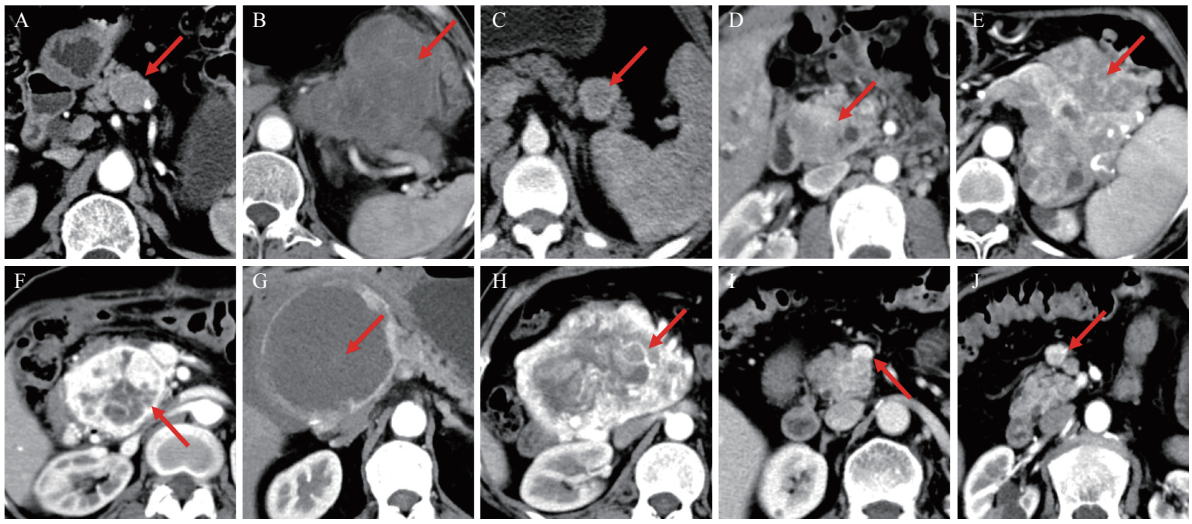

Fig. 3 **The imaging features of pancreatic neuroendocrine neoplasms on contrast-enhanced CT.** A: Regular tumor shape and iso-density in arterial phase. B: Irregular tumor shape and hypo-density in arterial phase. C: Well-defined tumor margin. D: Ill-defined tumor margin. E: Heterogeneous enhancement. F: Edge enhancement. G: Cystic or necrotic components. H: Intratumoral blood vessels. I: Vascular invasion. J: Lymph node metastases. CT: computed tomography.

bile duct dilatation as the diameter of more than 10 mm. Lymph node metastases were judged as positive when the short-axis diameter was more than 10 mm (***Fig. 3J***) and liver metastases were rated to be present if obvious metastatic lesions from the primary tumor were identified in the liver[11–14].

On visual inspection, the contrast enhancement pattern of the tumor was classified into hyperattenuation and iso- or hypo-attenuation when compared with that of normal pancreatic parenchyma. Attenuation values were measured to quantitatively evaluate the features of tumor enhancement in the arterial and portal phases. To avoid intratumoral features in which we were not interested (*e.g.*, cystic or necrotic components, biliary or pancreatic duct and calcification), we manually drew a round region of interest (ROI) of 30 mm^2 on the solid components of the tumor and normal pancreatic parenchyma. Attempts were made to place the ROI in the same site in both arterial and portal phases for each case. Tumor enhancement degree was defined as the HU of the tumor in each phase. The tumor-to-pancreas enhancement ratio was subsequently calculated as the HU value of the tumor divided by that of the normal pancreatic parenchyma in the arterial and portal phases, respectively. According to the different values of tumor attenuation, peak attenuation phase was observed either in arterial phase or portal phase[5–6,13].

Statistical analysis

Statistical analyses were performed using Stata/MP 13.1 for Windows (StataCorp LP, USA). The significance of differences among the three groups was assessed using chi-squared tests and one-way analysis of variance as appropriate. Multivariable logistic regression analysis was used to select the independent predictors. The cut-off points, areas under the curve (AUCs), sensitivities, and specificities for diagnostic performance were calculated using receiver operating characteristic (ROC) curve analysis. *P*-value <0.05 was considered to indicate statistical significance.

Results

Characteristics of all the 94 patients with PNENs are presented in ***Table 1***. There were 42 male and 52 female patients with age ranged from 19 to 81 years (54.14±12.55, mean±SD). Tumor size ranged from 6.5 to 121.4 mm (36.23±27.32, mean±SD). In terms of tumor location, more than half (56.4%) were found at the head or neck of the pancreas, and 43.6% at the body or tail of the pancreas. Based on the WHO 2017 classification, 39 tumors (41.5%) were PNENs G1, 42 (44.7%) were PNENs G2, and 13 (13.8%) were PNENs G3. Of the total cases, 90 diagnoses (95.7%) were based on surgical specimens and four (4.3%) on biopsies.

The data regarding CT imaging features of PNENs in correlation with tumor grade are summarized in ***Table 2***. The mean tumor size of PNENs G2 (45.93±32.56 mm) was significantly larger than that of G1 tumors (21.93±14.40 mm) (P<0.001), and PNENs G3 (47.80±19.17 mm) were larger than those with lower grades (P=0.005). All G3 patients and more than 3/4 of G2 patients (32/42) had tumors

Table 1 **Clinical features of all the 94 patients with PNENs**

Clinical features	Number of patients (%)
Age (years)	
Mean±SD	54.14±12.55
<55	48 (51.1)
≥55	46 (48.9)
Gender	
Male	42 (44.7)
Female	52 (55.3)
Tumor size (mm)	
Mean±SD	36.23±27.32
<20	35 (37.2)
≥20	59 (62.7)
Tumor location	
Head/neck	53 (56.4)
Body/tail	41 (43.6)
Tumor grade	
PNENs G1	39 (41.5)
PNENs G2	42 (44.7)
PNENs G3	13 (13.8)
Pathological source	
Surgery	90 (95.7)
Biopsy	4 (4.3)

PNENs: pancreatic neuroendocrine neoplasms.

larger than 2.0 cm in size. Irregular tumor shape was found in all G3 tumors demonstrating a significant difference from those of lower tumor grades (P<0.001). Meanwhile, more cases of G2 tumors (20/42, 47.6%) showed irregular shape than G1 tumors (8/39, 20.5%) (P=0.010). With regard to the tumor margin, PNENs G3 (12/13, 92.3%) were found more likely to show ill-defined margins than PNENs G1/G2 (P<0.001), while the difference between G1 (2/39, 5.1%) and G2 cases (7/42, 16.7%) was not significant (P=0.099). Likewise, more G3 (11/13, 84.6%) and G2 tumors (25/42, 59.5%) displayed heterogeneous enhancement patterns than did G1 tumors (15/39, 38.5%). There was a significant difference between G3 and those of relatively lower grades (P=0.018), but no significant difference between G1 and G2 (P=0.058). The presence of cystic or necrotic components was significantly more frequent in PNENs G2 (15/42, 35.7%) than in PNENs G1 (5/39, 12.8%, P=0.017), but no significant difference was found between PNENs G1/G2 and PNENs G3 (P=0.462). Intratumoral blood vessels and vascular invasion were more common in higher grades showing statistically significant differences between G1/G2 and G3 cases (P=0.027; P=0.001), as well as between G1 and G2 tumors (P=0.005; P=0.003). More cases of common bile duct dilatation were found in G3 tumors (5/13, 38.5%) than in G1/G2 tumors (P<0.001) and none were detected in PNENs G1, though there was no significant difference with respect to lower grade cases (P=0.089). Similarly, lymph node metastases and liver metastases were significantly associated with G3 tumors (P<0.001; P=0.001), while the difference between G1 and G2 tumors was not statistically significant (P=0.061; P=0.089).

When the tumor enhancement pattern by visual inspection was reviewed, iso- or hypo-attenuation was more frequently observed for PNENs G3 both in the arterial (11/13, 84.6%, P<0.001) and portal (11/13, 84.6%, P<0.001) phases, but they were not significantly different between lower grades (P=0.484; P=0.230). The quantitative CT attenuation values of PNENs were significantly lower in G3 tumors than in G1/G2 tumors both in the arterial phase (P=0.001) and portal phase (P=0.001) with no statistically significant differences between G1 and G2 tumors in either phase (P=0.369; P=0.899). The same trend was identified in terms of the tumor-to-pancreas enhancement ratio, in which the mean value in PNENs G3 was less than 1.00 and was significantly lower than that of G1/G2 tumors in arterial (P=0.002) and portal (P<0.001) phases, though there was no significant difference between lower grades (P=0.202; P=0.275).

By contrast, there were no significant differences among the three groups in terms of tumor location (P=0.881), edge enhancement (P=0.314), calcification (P=0.547), peak attenuation phase (P=0.317), and upstream pancreatic duct dilatation (P=0.274).

CT imaging features showing significant differences (P<0.01) between PNENs G3 and PNENs G1/G2 were selected for multivariable logistic regression analysis, including tumor size, shape, margin, vascular invasion, common bile duct dilatation, lymph node metastases, liver metastases, contrast enhancement pattern in the arterial and portal phases, tumor enhancement degree in both enhanced phases, and tumor-to-pancreas enhancement ratio in both enhanced phases. Results of multivariable stepwise logistic regression analysis showed ill-defined tumor margin was an independent predictor for differentiating PNENs G3 from PNENs G1/G2 (OR, 25.330; 95% CI, 2.839–226.074, P=0.004).

In the ROC analysis, ill-defined margin was a predictive factor of PNENs G3, with the largest AUC

Table 2 **Comparisons of CT imaging features between different tumor grades according to WHO 2017 classification in PNENs**

CT features	Group	Grade (WHO 2017)			*P*	*P**	*P***
		PNENs G1 (*n*)	PNENs G2 (*n*)	PNENs G3 (*n*)			
Tumor size (mm)	Mean±SD	21.93±14.40	45.93±32.56	47.80±19.17	<0.001	0.005	<0.001
	<20	25	10	0	<0.001	0.003	<0.001
	⩾20	14	32	13			
Location	Head/neck	21	24	8	0.881	0.686	0.765
	Body/tail	18	18	5			
Shape	Regular	31	22	0	<0.001	<0.001	0.010
	Irregular	8	20	13			
Margin	Well-defined	37	35	1	<0.001	<0.001	0.099
	Ill-defined	2	7	12			
Heterogeneity	Absent	24	17	2	0.010	0.018	0.058
	Present	15	25	11			
Edge enhancement	Absent	32	31	12	0.314	0.226	0.373
	Present	7	11	1			
Cystic or necrotic components	Absent	34	27	11	0.040	0.462	0.017
	Present	5	15	2			
Intratumoral blood vessels	Absent	38	32	8	0.003	0.027	0.005
	Present	1	10	5			
Vascular invasion	Absent	38	31	6	<0.001	0.001	0.003
	Present	1	11	7			
Calcification	Absent	37	37	12	0.547	0.909	0.278
	Present	2	5	1			
Enhancement pattern (arterial phase)	Hyper-	33	33	2	<0.001	<0.001	0.484
	Iso-/hypo-	6	9	11			
Enhancement pattern (portal phase)	Hyper-	29	26	2	<0.001	<0.001	0.230
	Iso-/hypo-	10	16	11			
Enhancement degree (HU), mean±SD	Arterial phase	110.78±33.72	118.95±33.77	81.75±40.54	0.005	0.001	0.369
	Portal phase	99.95±22.18	101.14±21.63	76.04±26.86	0.002	0.001	0.899
Tumor-to-pancreas enhancement ratio, mean±SD	Arterial phase	1.36±0.40	1.32±0.53	0.97±0.38	0.028	0.002	0.202
	Portal phase	1.26±0.25	1.22±0.29	0.96±0.34	0.005	<0.001	0.275
Peak attenuation phase	Arterial phase	24	32	8	0.317	0.585	0.154
	Portal phase	15	10	5			
Upstream pancreatic duct dilatation	Absent	32	28	9	0.274	0.714	0.114
	Present	7	14	4			
Common bile duct dilatation	Absent	39	39	8	0.003	<0.001	0.089
	Present	0	3	5			
Lymph node metastases	Absent	38	36	5	<0.001	<0.001	0.061
	Present	1	6	8			
Liver metastases	Absent	39	39	9	0.001	0.001	0.089
	Present	0	3	4			

CT: computed tomography; WHO: World Health Organization; PNENs: pancreatic neuroendocrine neoplasms; HU: Hounsfield units. *P**: PNENs G1/G2 *vs.* PNENs G3; *P***: PNENs G1 *vs.* PNENs G2. *P*-values were calculated using chi-square test.

of 0.906, a sensitivity of 92.3%, and a specificity of 88.9% (***Fig. 4A***). The AUC of other qualitative predictors ranged from 0.624 to 0.831, with the sensitivity ranging from 30.8% to 84.6% and the specificity ranging from 50.5% to 96.3%. With respect to quantitative features, when the optimal cutoff value of 0.98 was selected, portal enhancement ratio (PER) showed the best predictive accuracy for G3 tumors with an AUC of 0.855, sensitivity of 84.6%, and specificity of 86.4% (***Fig. 4B***). The cutoff value of 23.6 mm in tumor size showed an AUC of 0.747, sensitivity of 100.0%, and specificity of 49.4% for PNENs G3 prediction (***Fig. 4C***). Other quantitative parameters produced no better diagnostic value than PER in the study, with AUC, sensitivity, and specificity ranging from 0.809 to 0.824, 69.2% to 84.6%, and 80.3% to 93.8%, respectively (***Table 3***).

Discussion

The heterogeneity of PNENs is widely recognized in terms of clinical features, biological behaviors, and morphological characteristics presented in radiological and pathological examinations. Among the various features, tumor pathological grade was significantly related with the prognosis and treatment selection[3]. The development of radiological technology contributed to the increased incidence of PNENs[15]; however, reliable differentiation of tumor grade before treatment remains challenging. In the present study, we reviewed the qualitative and quantitative features of pretreatment contrast-enhanced CT imaging to identify CT features that predict tumor grade.

We found that CT imaging features, including tumor size, shape, cystic or necrotic components, intratumoral blood vessels, and vascular invasion, were significantly different between G1 and G2 tumors. With respect to the most aggressive G3 tumors, qualitative characteristics on contrast-enhanced CT imaging were observed that possessed differential diagnostic value with significant differences; these included tumor margin, heterogeneity, enhancement patterns in the arterial and portal phases, common bile duct dilatation, lymph node metastases, and liver metastases, as well as most of the features that were different between lower grades except for cystic or necrotic components. Tumor enhancement values and tumor-to-pancreas enhancement ratios in the arterial and portal phases were significantly lower in PNENs G3 than in PNENs G1/G2, highlighting the predictive value of these quantitative CT features.

Several previous studies have made efforts to investigate the predictive value of CT imaging features to identify PNENs G3. Kim *et al* reported that larger tumor size, lower arterial enhancement ratio (AER), lower PER, poorly-defined margin, bile duct dilatation, and vascular invasion were significant predictors for discerning G3 from G1/G2 tumors[12]. In their study, tumor size>3 cm showed a sensitivity of 92.3% and specificity of 66.9%, and PER <1.1 had a sensitivity of 92.3% and specificity of 80.5%. Guo *et al* found that larger size, ill-defined margin, lymph node invasion, and local invasion/vascular invasion/metastases were more commonly detected in PNENs G3 than in PNENs G1/G2[6]. AER and PER displayed the best diagnostic accuracy for G3 tumors. Likewise, Canellas *et al* reported that large tumor size and vascular invasion were more common in PNENs G3 than in PNENs G1/G2[16] and D'Onofrio *et al* found that tumor-to-pancreas enhancement ratios in the arterial and portal phases reliably identified G3

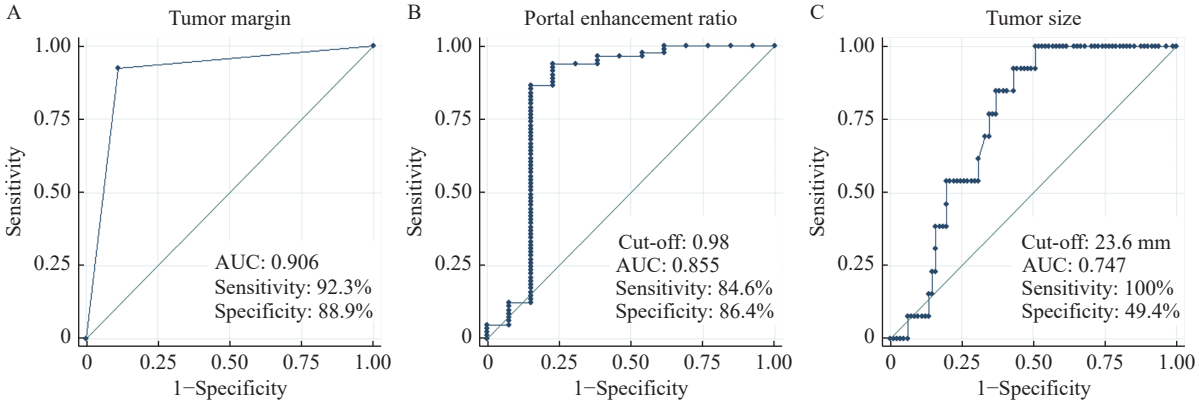

Fig. 4 **Receiver operating characteristic curve analysis of tumor margin, portal enhancement ratio, and tumor size for differentiating PNENs G3 from PNENs G1/G2.** A: Tumor margin. B: Portal enhancement ratio. C: Tumor size. AUC: area under the curve; PNENs: pancreatic neuroendocrine neoplasms.

Table 3 **Diagnostic performances of CT imaging features for differentiating PNENs G3 from PNENs G1/G2**

CT features	Sensitivity (%)	Specificity (%)	AUC	95% CI
Tumor size (mm)	100.0	49.4	0.747	0.692–0.802
Shape	100.0	65.4	0.827	0.775–0.879
Margin	92.3	88.9	0.906	0.823–0.989
Heterogeneity	84.6	50.6	0.676	0.560–0.792
Intratumoral blood vessels	38.5	86.4	0.624	0.482–0.767
Vascular invasion	53.9	85.2	0.695	0.549–0.841
Arterial enhancement pattern	84.6	81.5	0.831	0.720–0.941
Portal enhancement pattern	84.6	67.9	0.763	0.648–0.877
Arterial enhancement degree (HU)	69.2	92.6	0.809	0.675–0.943
Portal enhancement degree (HU)	69.2	93.8	0.815	0.682–0.948
Arterial enhancement ratio	84.6	80.3	0.824	0.713–0.935
Portal enhancement ratio	84.6	86.4	0.855	0.746–0.964
Common bile duct dilatation	38.5	96.3	0.674	0.535–0.813
Lymph node metastases	61.5	91.4	0.765	0.623–0.906
Liver metastases	30.8	96.3	0.635	0.503–0.768

The cut-off point of tumor size (mm), arterial enhancement degree (HU), portal enhancement degree (HU), arterial enhancement ratio, and portal enhancement ratio are 23.6, 73.12, 71.69, 1.06, and 0.98, respectively. CT: computed tomography; PNENs: pancreatic neuroendocrine neoplasms; AUC: area under the curve; CI: confidence interval; HU: Hounsfield units.

tumors in all cases[17]. Lower AER and early arterial enhancement value were revealed to be predictive factors for distinguishing G3 from G1/G2 tumors in reports by Horiguchi *et al*[18] and Kang *et al*[7]. These features were all covered in the present study, showing significant value of prediction, which paralleled the results of previous reports. Furthermore, our results suggested that ill-defined margin was an independent predictor for PNENs G3, showing the most powerful predictive value among all CT features, with an AUC of 0.906 and high sensitivity and specificity. In terms of quantitative features, PER <0.98 exhibited the largest AUC of 0.855 with good sensitivity and specificity. The diagnostic accuracy could be higher using a combination of the two features. The cutoff values of AER and PER were close to those of the previous report by Guo *et al*[6] further suggesting the effectiveness and reliability of these parameters for distinguishing G3 from lower grade tumors. Tumor size, the most common quantitative parameter, was related to tumor grades in most studies[18]. Nevertheless, the cutoff value of 23.6 mm for tumor size did not produce better diagnostic performance than did other predictive factors in our study, and this accorded with the findings of previous studies[18].

With the largest AUC for discerning PNENs G3, ill-defined tumor margin was significantly different between PNENs G3 and PNENs G1/G2; however, there was no significant difference between G1 and G2 tumors. We believe that this might be attributed to the more invasive growth pattern of the high grade G3 tumors, which was related to worse biological behavior and poorer prognosis.

Rich angiogenesis is common in the developmental process of many types of tumors and usually indicates poor prognosis[19–23]. Interestingly, the varying correlations between tumor vascularization and aggressiveness of PNENs were revealed in several studies[24–25]. Our results suggested that the mean enhancement values of tumors and tumor-to-pancreas enhancement ratios in the arterial and portal phases were all significantly lower in PNENs G3 than in G1/G2 tumors, in accordance with previous findings[18]. Angiogenesis could be assessed by calculating tumor microvascular density (MVD)[26]. Tumor-to-pancreas enhancement ratios were reported to reflect MVD, and lower MVD was also found in PNENs G3, hence the prediction of pathological grade *via* AER and PER was possible and reasonable[18].

Yamada *et al* reported that tumor size, margin, vessel involvement, and cystic or necrotic components were different between G1 and G2 tumors[27], which was partly affirmed by the present study where we found no difference of tumor margin between two lower grade groups though tumor margin showed high diagnostic performance for G3 lesions. Our finding in terms of tumor margin agreed with findings of studies

by Takumi *et al*[13] and Belousova *et al*[11] These studies demonstrated the usefulness of enhancement degree and tumor-to-pancreas enhancement ratio in identifying PNENs G2 from PNENs G1. Nevertheless, no significant differences of these features were detected between G1 and G2 in our series. This result is consistent with those of Guo *et al*[6] and D'Onofrio *et al*[17] The discrepancies among the results may be due to differences in the acquisition method and time of enhanced CT images, the distribution of study population included, and possibly the method of statistical analyses.

Recently, texture analysis was reported to be useful in the prediction of tumor grades[16,28]. By contrast, Guo *et al* demonstrated that texture features showed no better diagnostic performance than quantitative CT features such as AER and PER[6]. In the present study, tumor margin and PER both showed favorable diagnostic efficacy for PNENs G3. This suggests that traditional CT features still has substantial value for distinguishing G3 from lower grade tumors, as confirmed by the results of the present study.

Our study has several possible limitations. First, in all 13 PNENs G3 cases, five were PNETs G3, and eight were PNECs. PNENs G3 were not further divided into PNETs G3 and PNECs according to the WHO 2017 classification because of the small number of G3 tumors in the present study. Nevertheless, G3 tumors as a whole have been widely recognized with increased aggressiveness and poor prognosis[29–30]; therefore, the distinction of G3 from G1 and G2 tumors remains paramount. Second, inter-observer discrepancies were not determined because we used consensus judgment to minimize the error in subjective assessments. Further studies should assess the influence of subjective tendency and bias during imaging feature interpretation and ROI segmentation. Finally, several CT scanners were used in the examination and the differences between radiological facilities were not considered. Further studies with identical CT scanners should overcome this limitation.

In conclusion, our study revealed a close correlation between WHO classification and most of CT features except for tumor location, edge enhancement, calcification, peak attenuation phase, and pancreatic duct dilatation. The available features showed good values for discerning PNENs G3 from PNENs G1/G2. Of those, ill-defined tumor margin was an independent predictor for PNENs G3 with the largest AUC, while portal enhancement ratio showed the highest AUC in terms of quantitative features. Traditional contrast-enhanced CT continues to play a vital role in tumor grade differentiation and heterogeneity analysis prior to treatment. More prospective studies are warranted to validate our results.

Acknowledgments

This study was supported by a grant from the Innovation Capability Development Project of Jiangsu Province (No. BM2015004).

References

[1] Yao JC, Hassan M, Phan A, et al. One hundred years after "carcinoid": epidemiology of and prognostic factors for neuroendocrine tumors in 35, 825 cases in the United States[J]. *J Clin Oncol,* 2008, 26(18): 3063–3072.

[2] Reid MD, Balci S, Saka B, et al. Neuroendocrine tumors of the pancreas: current concepts and controversies[J]. *Endocr Pathol,* 2014, 25(1): 65–79.

[3] Ricci C, Casadei R, Taffurelli G, et al. WHO 2010 classification of pancreatic endocrine tumors. is the new always better than the old?[J]. *Pancreatology,* 2014, 14(6): 539–541.

[4] Inzani F, Petrone G, Rindi G. The new world health organization classification for pancreatic Neuroendocrine Neoplasia[J]. *Endocrinol Metab Clin North Am,* 2018, 47(3): 463–470.

[5] Kim JH, Eun HW, Kim YJ, et al. Pancreatic neuroendocrine tumour (PNET): Staging accuracy of MDCT and its diagnostic performance for the differentiation of PNET with uncommon CT findings from pancreatic adenocarcinoma[J]. *Eur Radiol,* 2016, 26(5): 1338–1347.

[6] Guo CG, Zhuge XL, Wang ZQ, et al. Textural analysis on contrast-enhanced CT in pancreatic neuroendocrine neoplasms: association with WHO grade[J]. *Abdom Radiol,* 2019, 44(2): 576–585.

[7] Kang J, Ryu JK, Son JH, et al. Association between pathologic grade and multiphase computed tomography enhancement in pancreatic neuroendocrine neoplasm[J]. *J Gastroenterol Hepatol,* 2018, 33(9): 1677–1682.

[8] Kulali F, Semiz-Oysu A, Demir M, et al. Role of diffusion-weighted MR imaging in predicting the grade of nonfunctional pancreatic neuroendocrine tumors[J]. *Diagn Interv Imaging,* 2018, 99(5): 301–309.

[9] Okabe H, Hashimoto D, Chikamoto A, et al. Shape and enhancement characteristics of pancreatic neuroendocrine tumor on preoperative contrast-enhanced computed tomography may be prognostic indicators[J]. *Ann Surg Oncol,* 2017, 24(5): 1399–1405.

[10] Toshima F, Inoue D, Komori T, et al. Is the combination of MR and CT findings useful in determining the tumor grade of pancreatic neuroendocrine tumors?[J]. *Jpn J Radiol,* 2017, 35(5): 242–253.

[11] Belousova E, Karmazanovsky G, Kriger A, et al. Contrast-enhanced MDCT in patients with pancreatic neuroendocrine tumours: correlation with histological findings and diagnostic

performance in differentiation between tumour grades[J]. *Clin Radiol,* 2017, 72(2): 150–158.

[12] Kim DW, Kim HJ, Kim KW, et al. Neuroendocrine neoplasms of the pancreas at dynamic enhanced CT: comparison between grade 3 neuroendocrine carcinoma and grade 1/2 neuroendocrine tumour[J]. *Eur Radiol,* 2015, 25(5): 1375–1383.

[13] Takumi K, Fukukura Y, Higashi M, et al. Pancreatic neuroendocrine tumors: Correlation between the contrast-enhanced computed tomography features and the pathological tumor grade[J]. *Eur J Radiol,* 2015, 84(8): 1436–1443.

[14] Luo YJ, Dong Z, Chen J, et al. Pancreatic neuroendocrine tumours: correlation between MSCT features and pathological classification[J]. *Eur Radiol,* 2014, 24(11): 2945–2952.

[15] Cappelli C, Boggi U, Mazzeo S, et al. Contrast enhancement pattern on multidetector CT predicts malignancy in pancreatic endocrine tumours[J]. *Eur Radiol,* 2015, 25(3): 751–759.

[16] Canellas R, Burk KS, Parakh A, et al. Prediction of pancreatic neuroendocrine tumor grade based on CT features and texture analysis[J]. *AJR Am J Roentgenol,* 2018, 210(2): 341–346.

[17] D'Onofrio M, Ciaravino V, Cardobi N, et al. CT enhancement and 3D texture analysis of pancreatic neuroendocrine neoplasms[J]. *Sci Rep,* 2019, 9(1): 2176.

[18] Horiguchi S, Kato H, Shiraha H, et al. Dynamic computed tomography is useful for prediction of pathological grade in pancreatic neuroendocrine neoplasm[J]. *J Gastroenterol Hepatol,* 2017, 32(4): 925–931.

[19] Bergers G, Benjamin LE. Tumorigenesis and the angiogenic switch[J]. *Nat Rev Cancer,* 2003, 3(6): 401–410.

[20] Ellis LM, Takahashi Y, Fenoglio CJ, et al. Vessel counts and vascular endothelial growth factor expression in pancreatic adenocarcinoma[J]. *Eur J Cancer,* 1998, 34(3): 337–340.

[21] Duarte IG, Bufkin BL, Pennington MF, et al. Angiogenesis as a predictor of survival after surgical resection for stage I non-small-cell lung cancer[J]. *J Thorac Cardiovasc Surg,* 1998, 115(3): 652–659.

[22] Weidner N, Folkman J, Pozza F, et al. Tumor angiogenesis: a new significant and independent prognostic indicator in early-stage breast carcinoma[J]. *J Natl Cancer Inst,* 1992, 84(24): 1875–1887.

[23] Vermeulen PB, Verhoeven D, Hubens G, et al. Microvessel density, endothelial cell proliferation and tumour cell proliferation in human colorectal adenocarcinomas[J]. *Ann Oncol,* 1995, 6(1): 59–64.

[24] Takahashi Y, Akishima-Fukasawa Y, Kobayashi N, et al. Prognostic value of tumor architecture, tumor-associated vascular characteristics, and expression of angiogenic molecules in pancreatic endocrine tumors[J]. *Clin Cancer Res,* 2007, 13(1): 187–196.

[25] Marion-Audibert AM, Barel C, Gouysse G, et al. Low microvessel density is an unfavorable histoprognostic factor in pancreatic endocrine tumors[J]. *Gastroenterology,* 2003, 125(4): 1094–1104.

[26] d'Assignies G, Couvelard A, Bahrami S, et al. Pancreatic endocrine tumors: tumor blood flow assessed with perfusion CT reflects angiogenesis and correlates with prognostic factors[J]. *Radiology,* 2009, 250(2): 407–416.

[27] Yamada S, Fujii T, Suzuki K, et al. Preoperative identification of a prognostic factor for pancreatic neuroendocrine tumors using multiphase contrast-enhanced computed tomography[J]. *Pancreas,* 2016, 45(2): 198–203.

[28] Choi TW, Kim JH, Yu MH, et al. Pancreatic neuroendocrine tumor: prediction of the tumor grade using CT findings and computerized texture analysis[J]. *Acta Radiol,* 2018, 59(4): 383–392.

[29] Basturk O, Yang ZH, Tang LH, et al. The high-grade (WHO G3) pancreatic neuroendocrine tumor category is morphologically and biologically heterogenous and includes both well differentiated and poorly differentiated neoplasms[J]. *Am J Surg Pathol,* 2015, 39(5): 683–690.

[30] Singhi AD, Klimstra DS. Well-differentiated pancreatic neuroendocrine tumours (PanNETs) and poorly differentiated pancreatic neuroendocrine carcinomas (PanNECs): concepts, issues and a practical diagnostic approach to high-grade (G3) cases[J]. *Histopathology,* 2018, 72(1): 168–177.